ACS Catalysis

Research Article

pubs.acs.org/acscatalysis

Effects of Electronic Perturbations on 1-Hexene Polymerization Catalyzed by Zirconium Amine Bisphenolate Complexes

D. Keith Steelman,[†] Silei Xiong,[‡] Grigori A. Medvedev,[‡] W. Nicholas Delgass,[‡] James M. Caruthers,*[,‡] and Mahdi M. Abu-Omar*[,†,‡]

[†]Brown Laboratory and the Negishi Brown Institute for Catalysis (NBIC), Department of Chemistry, Purdue University, 560 Oval Drive, West Lafayette, Indiana 47907, United States

[‡]School of Chemical Engineering, Purdue University, Forney Hall of Chemical Engineering, 480 Stadium Mall Drive, West Lafayette, Indiana 47907, United States

Supporting Information

ABSTRACT: The kinetics of 1-hexene polymerization using four zirconium amine bisphenolate catalysts, Zr[*t*Bu-ON^{X}O]-Bn$_2$ (where, X = pyr-CF$_3$ (**1**), pyr (**2**), pyr-CH$_3$ (**3**), pyr-OMe (**4**)) has been investigated to elucidate the effect of varying the electronic nature of the pyridine pendant ligand *X*. A model-based approach using a diverse set of data, including monomer consumption, evolution of molecular weight, and end-group analysis was employed to determine each of the reaction-specific rate constants involved in polymerization. The mechanisms of polymerization for **1**−**4** was similar, and the necessary elementary reaction steps included initiation, propagation, misinsertion, recovery from misinsertion, and chain transfer. It was observed that the electronic nature of the pendant pyridine ligand affects each monomer insertion event (propagation, misinsertion, and recovery) in a similar fashion, in concert with changes in the Hammett parameters of the ligand substituents. These findings underscore the importance of kinetic modeling to establish robust structure−activity relationships.

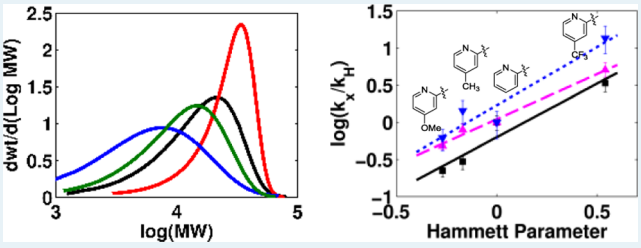

KEYWORDS: *zirconium, 1-hexene, polymerization, propagation, catalysis*

INTRODUCTION

A recent review of catalytic C−H functionalization highlights the importance of connecting the rational design of ligands with catalyst architecture to maximize activity and selectivity.[1] This concept is especially relevant to olefin polymerization because homogeneous single-site catalysts are amenable to exquisite control of the various kinetic steps through "catalyst design."[2−7] The demand for polyolefin materials continues to increase as the world's population grows.[8,9] Improved structure−activity relationships for single-site polymerization catalysts would have a direct impact on making desired polymer architectures.[10−13] A common view among chemists is that polymerization catalysts are beyond the reach of rational design.[14] This belief is built on the misconception that the promise of directly correlating kinetic constants to descriptors of the catalyst has not yet been realized, primarily as a result of the lack of proper quantitative kinetic analysis of all the relevant processes (i.e., kinetic steps) that comprise the olefin polymerization mechanism.[15,16]

A primary example is the obscure role of metal electrophilicity. On one hand, a highly electron-deficient complex has been proposed to interact more strongly with an incoming olefin.[17−19] Group IV complexes have shown enhanced activity with an increasingly electron-deficient metal center.[17] Another example is a series of Ni-based complexes bearing α-iminocarboxamide ligands.[20] For this family of catalysts, it was observed that systematically decreasing the electron density of the metal center resulted in increased activity toward ethylene polymerization.

On the other hand, it has been observed both experimentally[21,22] and theoretically[23,24] that electron-donating groups increase catalyst activity. Theoretical studies on a series of zirconium and titanium complexes with chelating alkoxide ligands showed that additional electron density on the metal center lowers the insertion barrier energy for an incoming olefin.[23,24] In addition, for a set of titanium bis(phenolate) catalysts, it was observed that electron-donating groups in the ligand increase activity.[21,22]

One specific family of nonmetallocene catalysts, pioneered by Kol and co-workers, utilizes an amine bisphenolate ligand system (see Figure 1).[25,26] The reason for choosing this particular family of ligands as part of our kinetic studies is the relative ease of synthesis and the ability to tune the catalyst's coordination environment.[27] Furthermore, these catalysts exhibit high activity, comparable to metallocene catalysts, for polymerization of 1-hexene in conventional organic solvents

Received: March 21, 2014
Revised: May 9, 2014
Published: June 5, 2014

   dx.doi.org/10.1021/cs5003788 | ACS Catal. 2014, 4, 2186−2190

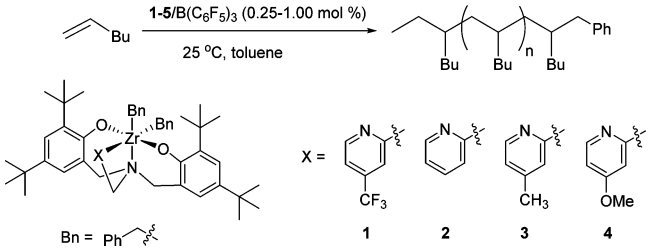

Figure 1. 1-Hexene polymerization catalyzed by zirconium amine bisphenolate complexes **1**−**4** when combined with the activator $B(C_6F_5)_3$.

such as toluene. This feature enables the collection of kinetic data in the condensed phase and eliminates potential mass transfer limitations that are inherent with gas phase monomers. Following up on Kol's earlier qualitative observations that the nature of the pendant ligand (X) and its distance from the metal center ($Zr-X$) influence chain transfer,[28] we have shown a correlation between the logarithm of the chain transfer rate constants, $k_{vinylidene}$ and $k_{vinylene}$, and the $Zr-X$ bond distance, which was established via quantitative kinetic modeling.[29] Furthermore, catalytic systems bearing a more electron-rich pendant exhibit a k_p several times lower than that for a less electron-rich catalyst. In this study, we will use quantitative kinetic modeling for a series of four Zr-based amine bisphenolate complexes bearing an electronically modified pyridine to elucidate the effect of electronic perturbations on the rate constants that comprise the olefin polymerization mechanism. In addition, we will examine the correlation of the determined rate constants with Hammett Parameters and computational results.

The complete kinetic analysis for system **2** has been reported previously.[29] Here we present a slightly modified (as described below) kinetic analysis for system **2** and the experimental data and complete kinetic analysis for 1-hexene polymerization of the structural analogues **1**, **3**, and **4**. For each system, we followed our previously developed kinetic modeling method[15,29,30] based on the analysis of multiresponse data. Within this analysis, each system is studied independently, and no a priori assumptions are made with respect to the elementary steps, as explained in detail in the Supporting Information. Using this procedure, a minimal set of elementary steps emerges, providing a fit to the data.

EXPERIMENTAL PROCEDURE

General Procedure. All manipulations were performed under dry inert atmosphere in a glovebox or at a vacuum manifold using air-sensitive techniques under N_2 or Ar atmosphere. Toluene and pentane were dried and degassed using a Solvent Drying System (Pure Process Technologies, LLC). Both solvents were stored over activated molecular sieves. Tetrabenzylzirconium was purchased from STREM and used as received. The monomer 1-hexene was purchased from Aldrich and purified by distillation over a small amount of dimethyl bis(cyclopentadienyl) zirconium and stored over molecular sieves. Tris(pentafluorophenyl) boron was purchased from STREM and purified by sublimation. Diphenylmethane was purchased from Aldrich and stored over molecular sieves. CH_3OD was purchased from Cambridge Isotopes and used as received. Toluene-d_8 was used as received and stored over molecular sieves. (4-Methylpyridin-2-yl)methanamine, (4-(trifluoromethyl) pyridin-2-yl)methanamine, and (4-methoxypyridin-2-yl) methanamine were purchased from Anichem, LLC, and used as received. ^1H and ^2H NMR experiments were performed on a Varian INOVA600 MHz or Bruker DRX500 MHz spectrometer.

The ligands and precatalysts (**1**−**4**) were prepared following modified literature procedures.[25,26,29,30] We describe herein the details for one representative procedure and provide the others in the Supporting Information (SI).

NMR Scale Polymerization of 1-Hexene with Zr[*t*Bu-ON^{Pyr}O]Bn$_2$ at 25 °C. The procedure for NMR scale polymerization is based on the literature.[29,30] For a typical polymerization, Zr[*t*Bu-ON^{Pyr}O]Bn$_2$ (6.1 mg, 0.0075 mmol) was dissolved in 0.5 mL of toluene in a small vial and sealed with a screw-cap septum. The vial containing the precatalyst solution was pierced with a 1 mL syringe. The vial and syringe were placed in a N_2 bag and allowed to equilibrate to 25 °C. Tris(pentafluorophenyl)boron (4.2 mg, 0.0083 mmol), 1-hexene (0.126 g, 1.50 mmol), and diphenylmethane (9.7 mg 0.058 mmol) were added to a 2 mL volumetric flask and diluted to the mark with toluene-d_8. This solution was placed in an NMR tube and sealed with a septum. The monomer/activator solution was placed in the spectrometer and allowed to equilibrate to 25 °C using a VT controller. A measurement was taken to determine the initial concentration of monomer relative to the internal standard. The NMR tube was removed from the spectrometer, and the catalyst precursor solution was added to the activator/monomer solution by piercing the septum while the syringe remained in the N_2 bag. The reaction mixture was allowed to shake for 30 s and inserted back into the spectrometer. Measurements were taken at predetermined time intervals until the reaction reached completion. This same sample was collected in a vial, cleaned up, and analyzed in accordance with the literature procedure.[16,29,30] NMR analysis shows that the resulting polymer produced with this catalyst is atactic.

Quenched NMR Scale Polymerization of 1-Hexene. The catalyst/activator and monomer/internal standard solutions were prepared in the same fashion as the previously described experiments using instead a temperature-controlled oil bath at 25 °C. These reactions were quenched at the time corresponding to the desired conversion of monomer using 0.75 mL of methanol-d_4. The quench reaction was analyzed by ^1H NMR to verify the conversion of monomer. This same sample was collected in a vial, cleaned up, and analyzed in accordance with the literature procedure.[16,29,30] The monomer conversion and the MWD of product of each quench reaction are given in Table 1.

Table 1. Kinetics Runs for 1-Hexene Polymerization with the Zr[*t*Bu-ON^{X}O]Bn$_2$/B(C$_6$F$_5$)$_3$ Catalysts 1−4[a]

	conversion (time/s), M_w, M_w/M_n		
X	run 1	run 2	run 3
pyr-CF_3 (**1**)	25% (80), 10k, 1.17	59% (205), 21k, 1.27	93% (515), 24k, 1.35
pyr (**2**)	47% (490), 16k, 1.34	71% (1259), 22k, 1.53	96% (3225), 20k, 1.87
pyr-Me (**3**)	26% (798), 8.6k, 1.26	55% (2051), 11k, 1.47	87% (5180), 12k, 1.62
pyr-OMe (**4**)	35% (1291), 7.9k, 1.58	44% (2355), 8.4k, 1.63	77% (6039), 8.7k, 1.72

[a]Catalyst = 3.0 mM, activator = 3.3 mM, and 1-hexene = 0.60 M.

dx.doi.org/10.1021/cs5003788 | ACS Catal. 2014, 4, 2186−2190

Table 2. Rate Constants for 1-Hexene Polymerization with the Zr[*t*Bu-ON^{X}O]Bn$_2$/B(C$_6$F$_5$)$_3$ Catalysts 1−4[a]

X	pyr-CF$_3$ (1)	pyr (2)	pyr-Me (3)	pyr-OMe (4)
Hammett parameter (σ)	0.54	0.00	−0.17	−0.27
k_i/M^{-1} s^{-1}	0.035	0.017 (±.02)	fast	fast
k_p/M^{-1} s^{-1}	4.5 (±0.4)	1.35 (−0.1/+0.2)	0.40 (±0.03)	0.3 (±0.01)
k_{mis} (10^{-3})/M^{-1} s^{-1}	39 (−5/+8)	7.7 (−0.4/+0.5)	6.1 (−0.5/+1.0)	3.7 (−0.2/+0.3)
k_{rec} (10^{-3})/M^{-1} s^{-1}	70 (−10/+20)	5.2 (−0.9/+1.2)	7.4 (−0.8/+1.5)	3.2 (−0.3/+0.4)
$k_{vinylidene}$ (10^{-3})/s^{-1}	1.24 (±0.02)	1.34 (−0.01/+0)	0.93 (±0.02)	1.24 (±0.01/)
$k_{vinylene}$ (10^{-3})/s^{-1}	0.99 (−0.02/+0.03)	0.441 (±0.003)	0.37 (±0.01)	0.294 (−0.006/+0.004)
cat. %	58% (−2%/+3%)	52%	58% (−3%/+2%)	47% (−0/+1%)

[a]Error estimation is based on the error in the GPC measurements where the details are given in the SI.

RESULTS

Although the complete kinetic analysis for catalyst **2** has been reported in a previous publication,[29] as explained below, this analysis has been modified slightly in the present paper. Here, we present the experimental data and a complete kinetic analysis for 1-hexene polymerization by catalysts **1**−**4**. For each system, we followed our previously developed kinetic modeling method[6,16,17] based on the analysis of multiresponse data that includes (1) monomer consumption, (2) MWDs at different conversions, (3) active site counts, and (4) vinyl end group counts. We determine the active site count as the number measured by quenching with methanol-d_4 and performing ^{2}H NMR measurement of the concentration of chains with deuterated end groups. The sites that have undergone 1,2-insertion are defined as primary sites, and the sites that have undergone 2,1-misinsertion are defined as secondary sites. Each system is studied independently and no a priori assumptions are made with respect to the elementary steps. The analysis procedure begins with the most basic mechanism, for example, initiation and propagation, and fitting is attempted to the entire data set; only after a simple mechanism is shown to fail is a new elementary step—for example, chain transfer—added and the fitting attempted again, etc.

This results in determination of a minimal set of elementary steps to fit the multiresponse data. For catalysts **1**−**4**, the minimal set includes:

(1) Initiation, which is generally fast because there is no induction period in the monomer consumption profiles for the monomer-to-catalyst ratios used;
(2) propagation via normal 1,2-insertion;
(3) 2,1-misinsertion and recovery from misinsertion, as supported by the measurement of the secondary active site;
(4) chain transfer via β-hydrogen elimination that results in the formation of vinylidene and vinylene end groups.

It is also noted that the catalyst participation is usually not 100% of the nominal precatalyst amount and may vary from system to system and from experiment to experiment for a given system. By catalyst participation, here, we mean the fraction of the precatalyst that is activated and initiated once the reactant species are combined. This is distinct from time-dependent deactivation. Catalyst participation for each system is determined via simultaneous fitting of the complete data set and is determined primarily by the active site counts and the location of the MWD peak. The value of catalyst participation is typically around 50% for the systems considered here. Although the degree of catalyst participation is not part of the catalytic mechanism, it can have an effect on the values of the rate constants obtained as a result of the kinetic modeling.

A case in point is catalyst **2**, for which we report rate constants that are somewhat different from those reported previously.[29] There are two reasons for the change in the values. First, the active site counts previously obtained for system **2** were based on batch scale experiments, which tend to be slightly lower than NMR scale experiments (45% vs 52%).[29,30] Second and more importantly, the vinyl counts reported in the previous paper[29] were scarce and showed significant scatter, resulting in higher uncertainty than desired. In the present study, all experiments for **2** and other systems were conducted on the NMR scale to eliminate inconsistency, and abundant data were collected to ascertain robust rate constants determination. Comparing the previously published constants[29] and the results in the present analysis herein shown in Table 2, the values of the rate constants have been corrected by the following amounts: k_p, −25%; k_{mis}, −75%; k_{rec}, −80%; $k_{vinylidene}$, −44%; $k_{vinylene}$, 52%. These results are consistent with the well documented[15,16,29,30] observation that not all of the catalyst participates in the polymerization, where the origin of the lack of 100% participation is not fully understood, and small differences in reaction conditions (e.g., batch vs NMR scale) can have some consequences.

The experimental data, along with the kinetic modeling fits of systems **1**−**4**, are shown in Figure 2. Additional fits to the active sites and vinyls counts are included in the SI. The values of the rate constants are shown in Table 2 including error bounds, which were determined using the methodology discussed previously[29] and in the SI.

DISCUSSION

In this study, the complete set of kinetic rate constants for four zirconium amine bisphenolate catalyst systems have been determined. The mechanism of 1-hexene polymerization for these catalysts consists of the following elementary reaction steps: initiation, normal propagation, misinsertion, recovery, and chain transfer.

The values of the rate constants are given in Table 2 Examining the summarized kinetic data in Table 2, the following conclusions emerge:

(1) On the basis of experimental active site counts, in all four systems, the catalyst participation is between 50% and 60%, with significant amounts of primary and misinserted secondary sites, where the former is slightly more prevalent than the latter. None of these systems exhibit a decrease in active site counts with time, indicating that there is no catalyst deactivation and the reinitiation after chain transfer is not slower than normal initiation.

(2) Examining the rate constants in Table 2, the rate constant for propagation increases with the electron-withdrawing capability of the pyridine substituent. This is due to the

dx.doi.org/10.1021/cs5003788 | ACS Catal. 2014, 4, 2186−2190

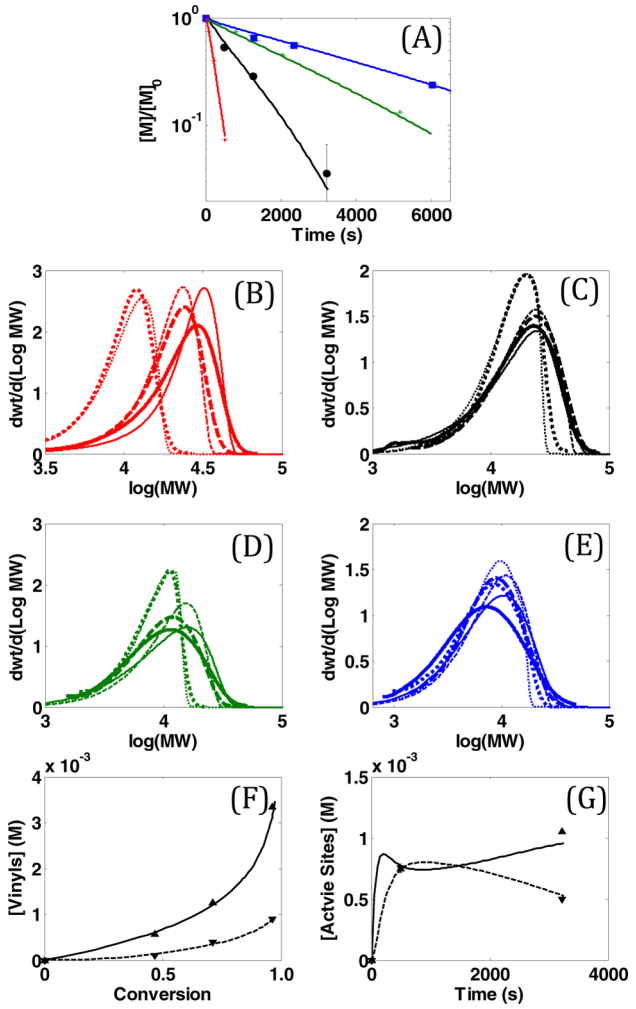

Figure 2. Multiresponse data set with fits for systems **1** (red), **2** (black), **3** (green), and **4** (blue) in the order of curves with decreasing slope in panel A. (A) Monomer consumption. Data, symbols; fits, lines. (B) MWDs at 25%, 59%, and 93% conversion for system **1**. (C) MWDs at 47%, 71%, and 96% conversion for system **2**. (D) MWDs at 26%, 55%, and 87% conversion for system **3**. (E) MWDs at 35%, 44%, and 77% conversion for system **4**. From B to E: data, thicker lines; fits, thinner lines. (F) End group analysis for system **2**. Vinylidene, up triangles (data)/solid line (fit); vinylene, down triangles (data)/dashed line (fit). Initial conditions: $[C]_0$ = 3.0 mM, $[M]_0$ = 0.60 M. (G) Active site counts of system **2**. Primary, up triangles (data)/solid line (fit); secondary, lower triangles (data)/dashed line (fit).

fact that the para position of the pyridyl pendant is electronically coupled to the active site via conjugation. The rate constants for the other monomer insertion steps, including misinsertion and recovery, exhibit a similar downward trend; the increase in the rate constant values for all three of these reactions is ∼1 order of magnitude from catalyst **4** to catalyst **1**.

(3) According to conclusion 2, the rate constant for initiation is expected to decrease from catalyst **1** to **4** if the rate-limiting step is a monomer insertion. In systems **1** and **2**, the k_p/k_i ratio is 129 and 79, respectively, which is large enough for k_i to be resolved from the MWD data. In systems **3** and **4**, the determination of k_i value is not possible because the data are not sensitive enough to changes in k_i, indicating that k_i is not slow enough relative to k_p. This suggests that the trend of decrease in k_i when going from catalyst **1** to **4** by the amount as large as the one observed for the other monomer-dependent steps does not hold. Our explanation for this is that the rate-limiting step for initiation is probably the displacement of the counterion, at which in the case of propagation, the counterion has already been displaced.

(4) Both of the rate constants for chain transfer, that is, $k_{vinylidene}$ and $k_{vinylene}$, are monomer-independent for all four systems and have a similar magnitude. As shown in Figure 3a,

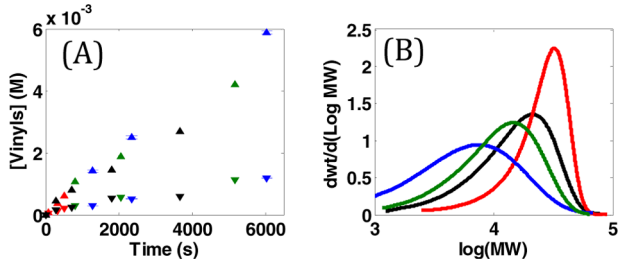

Figure 3. Collected data from catalysts **1** (red), **2** (black), **3** (green), and **4** (blue). (A) Concentration of vinyl end groups versus time (vinylidene, up triangles; vinylene, down triangles) and (B) MWDs at full conversion.

both the vinylidene and vinylene data for all four systems overlap when plotted versus time. However, because of the decrease in the propagation rate from catalyst **1** to **4**, the frequency of chain transfer with respect to propagation increases, causing the total amount of vinyls to increase and the MWD to become broader as the catalyst changes from **1** to **2** to **3** to **4**.

To summarize, with a change in the pyridine substituent group, we observe systematic changes in the rate constants of all the elementary steps involving monomer insertion and no changes in the rate constants of monomer-independent steps. Consequently, proper selection of the pyridine ligand enables the rational control of the MWD of the polymer (Figure 3b). To further quantify how the ligand structure affects the reaction rates, Hammett parameters are determined to quantify the electron withdrawing capabilities of different substituent groups. The structure−rate constant relationships are shown in Figure 4. The data presented in Figure 4 shows that electron-

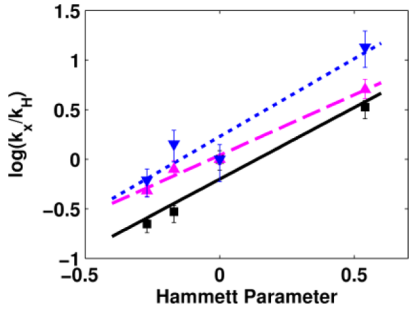

Figure 4. Plot of $\log(k_X/k_H)$ vs Hammett parameter. Squares, $\log(k_p)$; up triangles, $\log(k_{mis})$; down triangles, $\log(k_{rec})$. Lines are linear fits.

withdrawing substituents on the pyridine pendant increase the rate of all monomer-dependent steps with comparable Hammett constants: k_p (ρ = 1.45), k_{mis} (ρ = 1.22), k_{rec} (ρ = 1.57). This is likely the result of further destabilizing the already positive cationic active site by removing additional electron density, thereby making the active site more apt to react with available monomer. In addition to the correlation with the Hammett parameter, the rate constants are also correlated with

dx.doi.org/10.1021/cs5003788 | ACS Catal. 2014, 4, 2186−2190

various orbital energies, including the HOMO orbital as determined by DFT calculation (see SI).

CONCLUSIONS

A comprehensive kinetic study of four catalytic systems based on zirconium amine bisphenolate complexes has been completed, and the relevant rate constants and elementary reaction steps were determined for each system. The mechanism includes initiation, normal propagation, misinsertion, recovery, and chain transfer. The most significant finding was a correlation between the Hammett parameter and the rate constants of propagation, misinsertion, and recovery from misinsertion. Specifically, for catalysts **1**−**4**, the logarithm of the rate constants (k_p, k_{mis}, and k_{rec}) decrease with the electron-withdrawing capabilities of different substituent groups. This indicates that the systematic addition of electron-withdrawing character to the pendant results in a lowering of the energy barrier associated with each monomer insertion event. It was also noted that the chain transfer rates across catalysts **1**−**4** were relatively unaffected, indicating that the electronic nature of the pendant has little effect on chain transfer. A forthcoming study will explore the effect of steric perturbations on the rate of chain transfer.

ASSOCIATED CONTENT

Supporting Information

The synthesis of all ligands and precatalysts as well as a complete set of experimental procedures for each system and kinetic modeling material. This material is available free of charge via the Internet at http://pubs.acs.org.

AUTHOR INFORMATION

Corresponding Authors

*E-mail: caruther@purdue.edu.

*E-mail: mabuomar@purdue.edu.

Notes

The authors declare no competing financial interest.

ACKNOWLEDGMENTS

Financial support was provided by the U.S. Department of Energy by Grant No. DE-FG02-03ER15466. This research was supported in part by the National Science Foundation through TeraGrid resources provided by Purdue University under Grant No. TG-CTS070034N. Computing resources were also provided by Information Technology at Purdue.

REFERENCES

(1) Shul'pin, G. B. *Dalton Trans.* **2013**, *42*, 12794−12818.
(2) Chen, E. Y.-X.; Marks, T. J. *Chem. Rev.* **2000**, *100*, 1391−1434.
(3) Li, H.; Marks, T. J. *Proc. Natl. Acad. Sci. U.S.A.* **2006**, *103*, 15295−15302.
(4) Manz, T. A.; Phomphrai, K.; Medvedev, G.; Krishnamurthy, B. B.; Sharma, S.; Haq, J.; Novstrup, K. A.; Thomson, K. T.; Delgass, W. N.; Caruthers, J. M.; Abu-Omar, M. M. *J. Am. Chem. Soc.* **2007**, *129*, 3776−3777.
(5) Krauledat, H.; Brintzinger, H.-H. *Angew. Chem., Int. Ed. Engl.* **1990**, *29*, 1412−1413.
(6) Piers, W.; Bercaw, J. E. *J. Am. Chem. Soc.* **1990**, *112*, 9406−9407.
(7) Coates, G. W.; Waymouth, R. M. *J. Am. Chem. Soc.* **1991**, *113*, 6270−6271.
(8) Global Industry Analysts (GIA); *Plastics: A Global Outlook*; 2012;http://www.prweb.com/releases/plastics_bioplastics/engineered_plastics/prweb9194821.htm.
(9) Sita, L. R. *Angew. Chem., Int. Ed.* **2011**, *50*, 6963−6965.
(10) Angermund, K.; Fink, G.; Jensen, V. R.; Kleinschmidt, R. *Chem. Rev.* **2000**, *100*, 1457−1470.
(11) Bochmann, M. *J. Organomet. Chem.* **2004**, *689*, 3982−3998.
(12) Mohring, P. C.; Coville, N. J. *Coord. Chem. Rev.* **2006**, *250*, 18−35.
(13) Wang, B. *Coord. Chem. Rev.* **2006**, *250*, 242−258.
(14) Busico, V.; Cipullo, R.; Pellecchia, R.; Rongo, L.; Talarico, G.; Macchioni, A.; Zuccaccia, C.; Froese, R. D. J.; Hustad, P. D. *Macromolecules* **2009**, *42*, 4369−4373.
(15) Novstrup, K. A.; Travia, N. E.; Medvedev, G. A.; Stanciu, C.; Switzer, J. M.; Thomson, K. T.; Delgass, W. N.; Abu-Omar, M. M.; Caruthers, J. M. *J. Am. Chem. Soc.* **2010**, *132*, 558−566.
(16) Liu, Z.; Somsook, E.; Landis, C. R. *J. Am. Chem. Soc.* **2001**, *123*, 2915−2916.
(17) Warren, T. H.; Schrock, R. R.; Davis, W. M. *Organometallics* **1998**, *17*, 308−321.
(18) Ewart, S. W.; Sarsfield, M. J.; Williams, E. F.; Baird, M. C. *J. Organomet. Chem.* **1999**, *579*, 106−113.
(19) Tsukahara, T.; Swenson, D. C.; Jordan, R. F. *Organometallics* **1997**, *16*, 3303−3313.
(20) Azoulay, J. D.; Itigaki, K.; Wu, G.; Bazan, G. C. *Organometallics* **2008**, *27*, 2273−2280.
(21) Sernetz, F. G.; Mülhaupt, R.; Fokken, S.; Okuda, J. *Macromolecules* **1997**, *30*, 1562−1569.
(22) Porri, L.; Ripa, A.; Colombo, P.; Miano, E.; Capelli, S.; Meille, S. V. *J. Organomet. Chem.* **1996**, *514*, 213−217.
(23) Froese, R. D. J.; Musaev, D. G.; Matsubara, T.; Morokuma, K. *J. Am. Chem. Soc.* **1997**, *119*, 7190−7196.
(24) Froese, R. D. J.; Musaev, D. G.; Morokuma, K. *Organometallics* **1999**, *18*, 373−379.
(25) Tshuva, E. Y.; Groysman, S.; Goldberg, I.; Kol, M.; Goldschmidt, Z. *Organometallics* **2002**, *21*, 662−670.
(26) Tshuva, E. Y.; Goldberg, I.; Kol, M.; Goldschmidt, Z. *Organometallics* **2001**, *20*, 3017−3028.
(27) Kerton, F. M.; Holloway, S.; Power, A.; Soper, R. G.; Sheridan, K.; Lynam, J. M.; Whitwood, A. C.; Willans, C. E. *Can. J. Chem.* **2008**, *86*, 435−443.
(28) Groysman, S.; Goldberg, I.; Kol, M.; Genizi, E.; Goldschmidt, Z. *Organometallics* **2003**, *22*, 3013−3015.
(29) Steelman, D. K.; Xiong, S.; Pletcher, P. D.; Smith, E.; Switzer, J. M.; Medvedev, G. A.; Delgass, W. N.; Caruthers, J. M.; Abu-Omar, M. M. *J. Am. Chem. Soc.* **2013**, *135*, 6280−6288.
(30) Switzer, J. M.; Travia, N. E.; Steelman, D. K.; Medvedev, G. A.; Thomson, K. T.; Delgass, W. N.; Abu-Omar, M. M.; Caruthers, J. M. *Macromolecules* **2012**, *45*, 4978−4988.